JOURNAL OF MATERIALS SCIENCE 26 (1991) 1775–1780

The effect of microstructure on residual stress-producing and -releasing mechanisms in ceramics processing

GUO MIAN*, T. YAMAGUCHI
Laboratory of Materials Science, Faculty of Science and Technology, Keio University, Yakohama 223, Japan

A new non-destructive method has been developed for determining the internal stress of ferroelectric and ferromagnetic ceramic materials by comparing the relative changes in the permeability of the materials. The first experimental data of the relationship between the residual stress and the microstructure of the ceramic material has been obtained by this method. Residual stress-producing and -releasing behaviours in Ni–Cu–Zn ceramics processing depends on the microstructure of these materials. The experimental results show that more residual stress is produced in quenching and released in annealing for a sample with a lower density, smaller grain sizes and a higher pore fraction. Whether or not the residual stress in a quenched Ni–Cu–Zn ceramic sample is released back to its initial as-sintered state through an annealing process depends upon the microstructure. The stress produced by air-quenching was almost completely released by the annealing process when the relative densities of the samples were lower than 83%. However, the stress-releasing effect decayed rapidly with increasing density when the relative densities of the samples were higher than 94%. On the other hand, the residual stress in the Ni–Cu–Zn ceramics rose very rapidly when the air-quenching temperature was higher than 830 °C. The stress was estimated by considering the effect of magnetostriction on the initial magnetization process in the materials. A simple theoretical model has been developed to interpret the results.

1. Introduction

The residual stress in ceramic materials affects not only their electric and magnetic properties but also their mechanical properties. Mechanical properties are important for the use of ceramic materials in solid-state applications, such as integrated circuit substrate, piezoelectric sensors, and magnetic cores. The idea of the ceramics engine also demands a maximum reduction of the internal stress of ceramic materials under different working temperatures and heating–cooling rates. As a result of modern applications of ceramic materials, there is a much greater need to take into account the relationship between residual stress and the microstructure of ceramic materials. However, generally speaking, the average grain size of ceramic materials is greater than the wavelength of X-rays, so one looses the accuracy of the determination of lattice spacing by X-ray diffraction (XRD). Therefore, it is very difficult to determine the residual stress of ceramic materials by XRD which is widely used in metal stress analysis. This situation results in some difficulties in understanding the relationship between microstructure and residual stress in ceramic materials.

We investigated the effect of the microstructure on stress-producing and -releasing mechanisms of Ni–Cu–Zn magnetic ceramic materials by comparing relative changes in the permeability of the materials before and after quenching, as well as, before and after annealing, and estimated the difference in the microstructure through scanning electron microscope (SEM) observations. In particular, we investigated the effects of microstructure properties such as density and pore fraction on the stress-producing and -releasing processes, and the relationship between residual stress and quenching temperature in Ni–Cu–Zn ferrite processing. Since the magnetic and non-magnetic ceramic materials are both processed by sintering and have many properties such as microstructure, grain boundaries, and pore fraction in common, the results of this experiment are very important in ceramics processing. We are not only interested in the residual stress in Ni–Cu–Zn ceramic material in particular, but also in the residual stress in ceramic materials in general. The residual stress was determined by a calculation based on the assumption that the magnetization process for initial magnetization

* *Present address*: Department of Electrical Engineering, Washington University, St. Louis, MO 63130, USA. Supported in part by The Computer and Communication Promotion Foundation, NEC, Japan (C & C Foreign Researcher Award, 1987).

0022–2461/91 $03.00 + .12

was a rotation process. This assumption had been confirmed by our previous experimental findings [1]. The data obtained by this experiment is the first data on the relationship between residual stress and microstructure of the ceramic material.

2. Experimental procedure

Fig. 1 illustrates the basic structure of the experiment. The residual stresses were produced by an air-quenching process and then released by an annealing process. The stress was calculated from the relative changes of the permeability of the sample with respect to its initial unstressed state, to be discussed in the following pages.

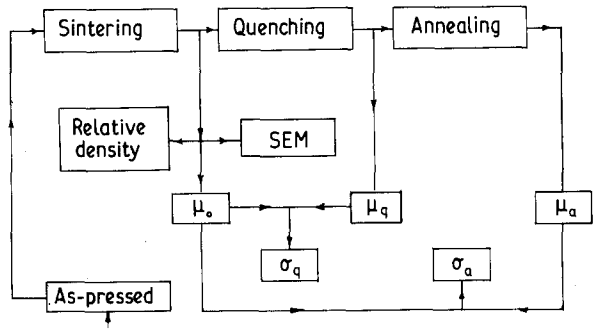

Figure 1 The block diagram of the experiment. σ_q and σ_a are corresponding to the residual stresses after quenching and annealing, respectively. The stresses are estimated by comparing the relative changes in the permeability of the samples. μ_q and μ_a are the permeabilities of the as-quenched and as-annealed samples, respectively. μ_0 is the permeability of the samples just after sintering.

2.1. Sample preparation

Pre-sintered powder containing CuO, NiO, ZnO and Fe_2O_3 in a molar ratio of 6:12:33:49 was mixed with 1 wt % polyvinyl alcohol (PVA) and pressed for one min at a different pressure for each sample. The size of the pressed sample was 7:11:45 mm (t:h:w). The samples were toroidal to eliminate the demagnetization effect. Each sample was sintered at a different temperature between 1000 and 1150 °C in order to obtain a different microstructure. The cooling process was divided into several steps to minimize the residual stress produced by the cooling process. The sintering procedure is shown in Fig. 2a.

2.2. Air-quenching process: stress-producing

The sintered samples were heated again to 900 °C at a heating rate of 150 °C h^{-1}, the same as was used in the sintering process. Each of them was held at a different temperature (= quenching temperature, up to 900 °C) for 30 min and then taken into a room temperature air-pumped zone. We found that it was difficult for the sintering process to occur in Ni–Cu–Zn materials for a heating temperature lower than 950 °C, so that the quenching temperatures were designed to be up to 900 °C to avoid the changes of magnetic properties due to the growth of the grains. The residual stress was created by this quenching process because the different cooling rates inside and outside of the materials brought about the temperature gradient, which resulted in strain in the materials. Since there are many pores and grain boundaries in ceramic materials, the ceramic materials are much different from single crystals. The residual stress in a single crystal is mainly caused by dislocations or phase transitions in the crystal. However, in comparing the number of dislocations on the surface of a grain with the number of dislocations in the grain for ceramic materials, there is a much greater number of dislocations on the surface of the grain. Consequently, the stress in ceramic materials strongly depends on the microstructure of the materials such as grain size, pore fraction and grain boundaries. There is no such effect for single crystals. Although a different cooling rate might result in phase transitions in the material, XRD analysis indicated that both the quenched and the annealed samples have the spinel structure, the same phase as the as-sintered sample. In comparing the quenched

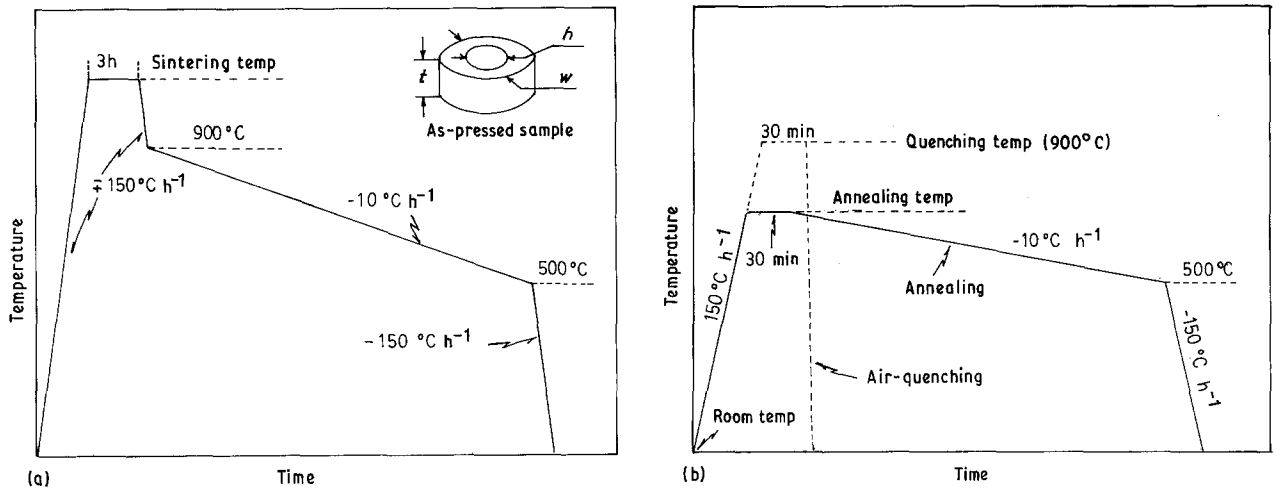

Figure 2 (a) The sintering procedure. The sample was sintered at a designated temperature between 1000 and 1150 °C in order to obtain a different microstructure for each sample. (b) The air quenching and the annealing procedures. The maximum quenching temperature was set at 900 °C to avoid the changes in magnetic properties due to the growth of grains. The cooling steps in the annealing were the same as those in the sintering procedure.

and annealed samples with the samples before quenching, no phase transition was detected.

2.3. Annealing process: stress-releasing

The air-quenched sample was heated again at a heating rate of 150 °C h^{-1} and held at a designated annealing temperature for 30 min, then cooled by the same process as in sintering. The annealing procedure is illustrated in Fig. 2b. The highest annealing temperature was set at 900 °C, the same as the highest quenching temperature.

3. Stress evaluation

It has been revealed by our experiments that the magnetization of Ni–Cu–Zn ceramic materials in a weak field is a rotation process [1]; therefore it is possible to estimate the residual stress by an analysis of this process [2, 3].

Generally speaking, for an unstressed sample, the magnetization vector is along the easy-magnetization direction of the material when the applied field is zero. The easy-magnetization direction for the Ni–Cu–Zn ferrite with a cubic structure is ⟨1 0 0⟩. To simplify the problem, we assume that the direction of the stress produced by quenching on a toroidal sample is approximately parallel to that of the applied field. Let the angle between the easy-magnetization direction, ⟨1 0 0⟩, and the magnetization of the materials be ϕ, and the angle between the applied field and the ⟨1 0 0⟩ direction is θ, as shown in Fig. 3. According to ferromagnetism theory, the total energy of the system is given by

$$E = -3/2\lambda_s\sigma\cos^2(\theta-\phi) + K_1\sin^2\phi\cos^2\phi - HM_s\cos(\theta-\phi) \quad (1)$$

Where λ_s is the magnetostriction of the material, K_1 the magnetic anisotropic constant of the material, M_s the saturation magnetization, and σ the stress parallel to the direction of the applied field H. At an equilibrium state, $\partial E/\partial\phi = 0$ yields

$$H = \frac{K_1\sin(4\phi) - 3\lambda_s\sigma\sin 2(\theta-\phi)}{2M_s\sin(\theta-\phi)} \quad (2)$$

Since $M = M_s\cos(\theta-\phi)$, then the magnetic susceptibility χ_a is

$$\chi_a = \frac{\partial M}{\partial H} = \frac{\partial M}{\partial\phi}\frac{\partial\phi}{\partial H} = M_s\sin(\theta-\phi)\frac{\partial\phi}{\partial H} \quad (3)$$

and

$$\frac{\partial H}{\partial\phi} = \frac{[2K_1\cos(4\phi) + 3\lambda_s\sigma\cos2(\theta-\phi)]\sin(\theta-\phi) + \frac{1}{2}[K_1\sin(4\phi) - 3\lambda_s\sigma\sin2(\theta-\phi)]\cos(\theta-\phi)}{M_s\sin^2(\theta-\phi)} \quad (4)$$

Since we consider only the initial magnetization process, the applied field is very small, so the angle between the magnetization and ⟨1 0 0⟩ is very small; that is

$$\phi(H\to 0)\to 0$$

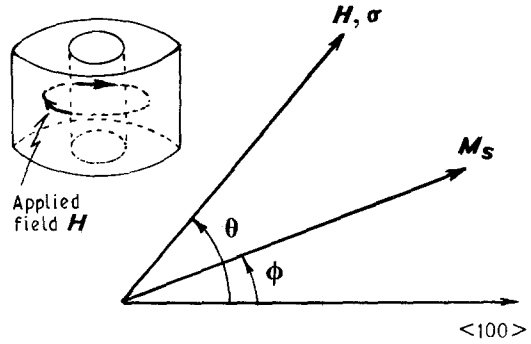

Figure 3 The magnetization process of the materials under a stress σ parallel to the applied field H. For the initial magnetization process, the applied field is very small so that the magnetization vector tends to stay in the easy-magnetization direction ⟨1 0 0⟩ for cubic structure materials. The direction of the applied field is always parallel to the tangential direction of the circle in the plane slicing the toroidal samples.

which yields

$$\frac{\partial H}{\partial\phi} = \frac{2K_1 - 3\lambda_s\sigma\sin^2\theta}{M_s\sin\theta} \quad (5)$$

For real polycrystals, the grains are randomly oriented. Therefore, $\sin^2\theta$ has to be replaced by the average value of the $\sin^2\theta = 2/3$. Thus, substituting the above results into Equation 3, we get the initial magnetic susceptibility

$$\chi_a = \frac{M_s^2}{3(K_1 - \lambda_s\sigma)} \quad (6)$$

Since the initial permeability is $\mu = 4\pi\chi_a + 1$, and for high permeability materials, $\mu \gg 1$, we get approximately

$$\mu_T/\mu_0 = (K_1 - \lambda_s\sigma_0)/(K_1 - \lambda_s\sigma_T) \quad (7)$$

Where μ_0 is the measured permeability of the sintered sample. μ_T, which depends on the residual stress in the measured sample, can be the measured permeability of either the quenched or the annealed sample. σ_T can be the residual stress of either the quenched or the annealed sample. We assume that in an as-sintered sample the residual stress σ_0 was largely reduced by a well-designed cooling process, so that the stress in the as-sintered sample during the magnetization process is approximately equal to the stress due to the magnetostriction of the material. That is

$$|\lambda_s\sigma_0| \approx \lambda_s^2 E \quad (8)$$

where E is the Young's modulus of the material. K_1 of the material was about 10^2 J cm^{-3}, the magnetostriction was -3.4×10^{-6}, and E was about 10^{11} N m^{-2}. Since $K \gg \lambda_s^2 E$, finally we get

$$\sigma_T \approx -(\mu_0/\mu_T - 1)K_1/\lambda_s = -(\mu_0/\mu_T - 1)/\lambda_s \times 10^2\,\text{Pa} \quad (9)$$

Thus the residual stress in the quenched or annealed sample can be calculated from μ_0 and μ_T, the measured permeabilities of the sample before and after quenching or annealing.

4. Results and discussion

Fig. 4 indicates that the residual stress depends on the air-quenching temperature. The stress in the as-quenched samples increased sharply for a quenching temperature greater than 830 °C. Cracks were frequently found in the samples when the quenching temperatures were higher than 1100 °C. The stress at which the material fractures was determined to be about 35 MPa by a mechanical test. This was very close to the result obtained by magnetic measurements, shown in Fig. 4. This result indicates that our assumptions and approximations were reasonable.

Fig. 5 shows the dependence of residual stress upon relative density for the as-quenched Ni–Cu–Zn ferrite when the quenching temperature was fixed at 900 °C. Fig. 6 is a scanning electron microscopy (SEM) observation of the relationship of density to microstructure. The residual stress was decreased by increasing the relative density, lowering the pore fraction and raising the grain sizes of the materials. This result may be explained by considering the different heat expansion coefficients corresponding to different densities of the materials. In general, there are gas phases, such as pores, in ceramic materials. Let us consider a *quasi*-static process of changing the temperature of a material without forming a fracture. Assume the volume expansion coefficient of the grains is β_g, the volume expansion coefficient of the pores is β_p, and the average volume expansion coefficient of the material is β_r. Also assume all stresses applied to the grains are either pure tensile or compressive stresses. So, for a *quasi*-static infinitesimal change of the temperature of

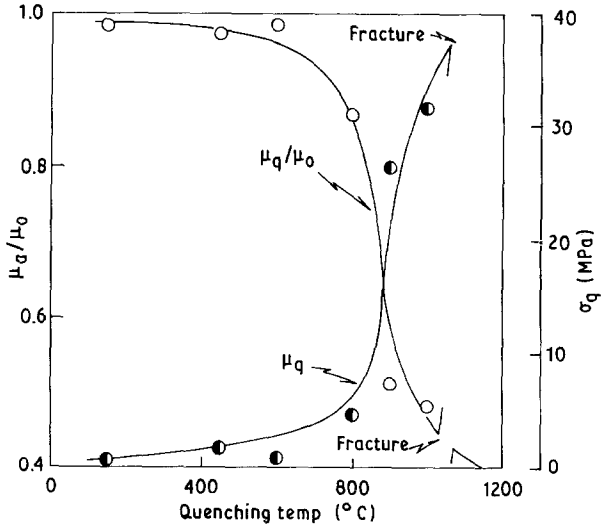

Figure 4 The residual stress and quenching temperature dependence of the Ni–Cu–Zn ceramic materials. The samples were sintered at 1200 °C for 2 h and then cooled by the cooling procedure illustrated in Fig. 2a. Each sample was heated again and held at the designated quenching temperature for 30 min, then cooled by an air pump. The permeability of the unstressed as-sintered sample was 1300.

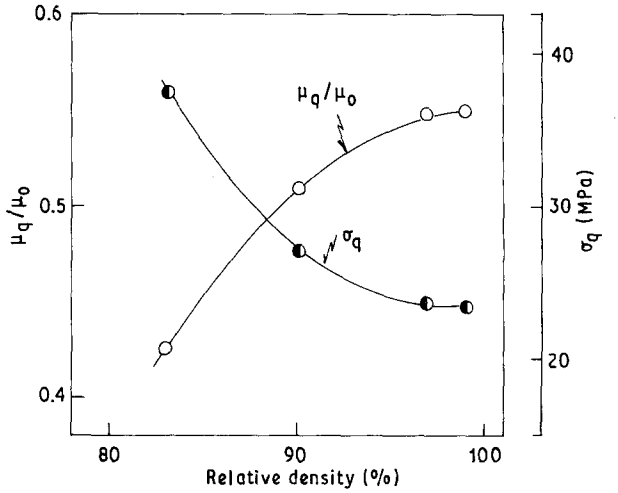

Figure 5 The residual stress produced by quenching depends on the density of the material. The quenching temperature was fixed at 900 °C.

the system, the stress applied to the ith grain is

$$\sigma_{gi} = \kappa_g(\beta_r - \beta_g)\Delta T_{gi} \tag{10a}$$

The stress applied to the air-phase in the jth pore is

$$\sigma_{pj} = \kappa_p(\beta_r - \beta_p)\Delta T_{pj} \tag{10b}$$

Where κ_g and κ_p are the elastic constants of the grains and pore (or gas) phases, respectively. ΔT_{gi} is the temperature change of the ith grain, and ΔT_{pj} is the temperature change of the jth pore. The stress in the sample is an internal force and therefore its summation should be zero under an equilibrium state, that is

$$\sum_i^{N_g} \sigma_{gi}\Delta V_{gi} + \sum_j^{N_p} \sigma_{pj}\Delta V_{pj} = 0 \tag{11}$$

yielding,

$$\kappa_g(\beta_r - \beta_g)\sum_{i=1}^{N_g} V_{gi}\Delta T_{gi} + \kappa_p(\beta_r - \beta_p)\sum_{j=1}^{N_p} V_{pj}\Delta T_{pj}$$
$$= \kappa_g(\beta_r - \beta_g)\Delta T\sum_i^{N_g} V_{gi} + \kappa_p(\beta_r - \beta_p)\Delta T\sum_j^{N_p} V_{pj} = 0 \tag{12}$$

Where we have assumed that the number of grains and pores are N_g and N_p, respectively, and V_{gi} is the volume of the ith grain, and V_{pj} the volume of the jth pore. Since we have assumed that the change of the temperature was approximately a *quasi*-static equilibrium process, we replaced ΔT_{gi} and ΔT_{pj} by ΔT, the change of the temperature of the system in the above calculation. Let

$$V_g = \sum_{i=1}^{N_g} V_{gi} \tag{13}$$

$$V_p = \sum_{j=1}^{N_p} V_{pj} \tag{14}$$

Substituting the above two equations into Equation 12 we get

$$\beta_r = \frac{\kappa_g\beta_g V_g + \kappa_p\beta_p V_p}{\kappa_g V_g + \kappa_p V_p} \tag{15}$$

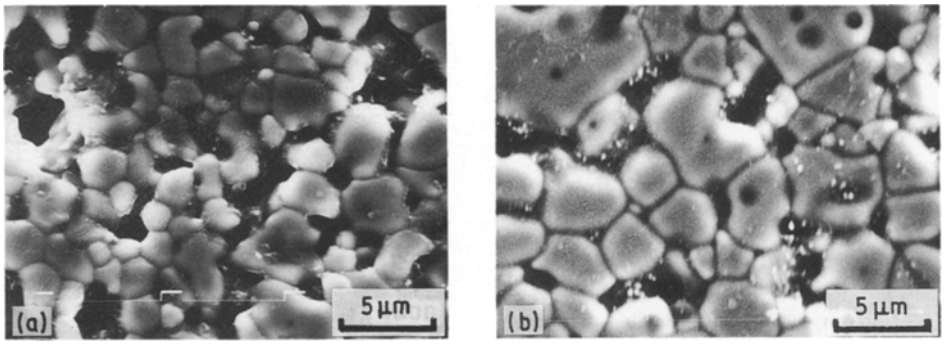

Figure 6 SEM of Ni–Cu–Zn ceramic materials. Low density corresponds to a high pore fraction and small grain sizes. (a) The sample was pressed at 3.9 GPa and sintered at 1000 °C. The average grain size and the relative density of the sample are 2 μm and 83%, respectively. (b) The sample was pressed at 6.5 GPa and sintered at 1050 °C. The average grain size and the relative density of the sample are 4 μm and 97%, respectively.

Considering that the volume fraction of the pores in the material is very small, and that the elastic constant of the grains is much larger than that of the gas phase, we get

$$\beta_r = \frac{(\beta_g \kappa_g V_g + \beta_p \kappa_p V_p)\left(1 - \dfrac{\kappa_p V_p}{\kappa_g V_g}\right)}{\kappa_g V_g} \tag{16}$$

In the above calculation, we expanded β_r in a Taylor expansion and then neglected the terms

$$\frac{\left(\dfrac{\kappa_p V_p}{\kappa_g V_g}\right)^n [\kappa_g \beta_g V_g + \kappa_p \beta_p V_p]}{\kappa_g V_g} \tag{17}$$

for $n \geq 2$. On the other hand, since the volume expansion coefficient of the gas is greater than that of the grains, finally we get

$$\beta_r = \beta_g + C V_p / V_g \tag{18}$$

where

$$C = (\beta_p - \beta_g)\kappa_p / \kappa_g > 0$$

From the term expressed as CV_p/V_g in Equation 18, we see that the average heat expansion coefficient of the materials is increased linearly by increasing in the volume fraction of pores when $V_g \gg V_p$ is satisfied. We have obtained some results which can be used for the explanation of the experimental results as follows: As a result of the fact that the heat conductivity of any solid is larger than that of any gas, the conductivity of the material is lowered by increasing its pore fraction. Heat transfer is restricted by the pores, bringing about larger temperature gradients in the material in both the cooling and heating processes for lower density samples. On the other hand, as we have derived in Equation 18, for $V_g \gg V_p$, the higher the pore fraction, the higher the thermal expansion coefficient. Consequently, larger local stresses would be created for the samples with higher pore fractions because the stress is proportional to the temperature gradient and the expansion coefficient. In fact, during the quenching and heating processes, the expansion coefficient of the sample is no longer independent of the temperature. It can be shown that

$$\beta_r \simeq \beta_g + C \frac{\sum_j^{N_p} V_{pj} \Delta T_{pj}}{\sum_i^{N_g} V_{gi} \Delta T_{gi}}$$

However, β_r is still related to the pore fraction and temperature gradient of the material. The qualitative conclusion in reality will not be changed from that of the simple model. In conclusion, higher residual stresses correspond to higher pore fractions and lower densities. Thus, the experimental results of the quenched samples shown in Figs 5 and 6 are explained.

It is interesting that whether the residual stress in the quenched sample is released back to its initial state (as-sintered state) or not by the annealing process depends on its microstructure. Fig. 7 shows the experimental results. The stress produced by the air-quenching process was almost completely released for the sample with relative density of 83%. The releasing effect decayed sharply when the relative density was higher than 94%.

Fig. 8 gives similar results with respect to the annealing temperature. The results may be understood by the following interpretation: In general, high temperature provides a large driving force to lower the energy by reducing dislocations in materials. Therefore, for a certain heating period, the dislocations of the materials may be reduced by raising the heating temperature. On the other hand, higher pore fractions result in more dislocations on the grain boundaries, and smaller grain sizes bring about higher surface energies of the grains. These cause higher potential energies on the grain boundaries. Therefore, the reduction in the number of dislocations during the annealing process is greater for lower density samples than for higher density samples. And since a heavy dislocation corresponds to a high microstress, reducing this potential energy brings about the stress-releasing process during the annealing process. Another explanation for the results, is that, since the direction of the thermal stress due to heating is opposite to that of the stress due to the cooling process, the stress due to heat expansion in the annealing process accelerates the release of stress produced by the air-quenching process. Consequently, lower density samples correspond to larger stress-releasing forces in the

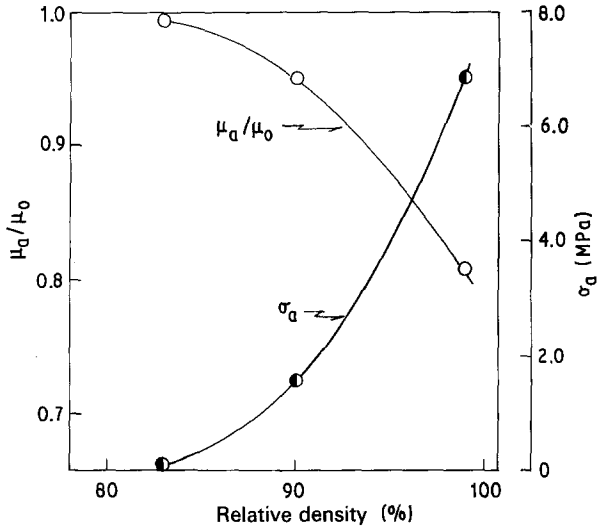

Figure 7 The residual stress is more easily released by the annealing process for samples with lower densities. The releasing effect decays rapidly when the relative density of the material is higher than 94%. The annealing temperature was fixed at 900 °C, the same as the quenching temperature.

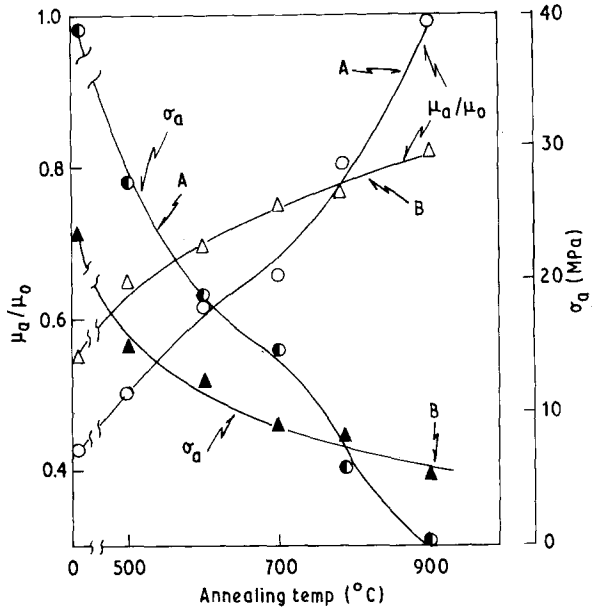

Figure 8 The stress releasing effect versus the annealing temperature of the materials. The samples were quenched at 900 °C. Samples A and B were sintered at 1000 and 1050 °C with relative densities of 83 and 98%, respectively.

annealing process. The results shown in Figs 7 and 8 can now be understood.

As we mentioned previously, the stress obtained by the magnetic measurement agrees with the result of a mechanical test. If there was any phase transition (even in a very small fraction), the permeability of the materials would be decreased much faster than the observed result shown in Fig. 4. In addition, no phase transition could be found from XRD. Consequently, we do not consider the stresses due to the phase transitions here.

5. Conclusions

1. The microstructure effect on residual stress-producing and- releasing processes in ceramics processing was investigated by a non-destructive stress evaluation method using magnetic measurements. Both the residual stress-producing and -releasing processes occur more easily in the samples with lower densities, smaller grain sizes and higher pore fractions.

2. Whether or not the residual stress in the quenched sample is released back to its initial as-sintered state by an annealing process depends on the microstructure of samples. For the Ni–Cu–Zn ceramic material, the stress due to the air-quenching was almost completely released by the annealing process for the samples with relative density lower than 83%, while the stress-releasing effect decayed rapidly for the samples with relative densities higher than 94%.

3. The residual stress in the Ni–Cu–Zn ceramic materials rose very sharply when the air-quenching temperature was higher than 830 °C. This result is very useful for minimizing the stress produced by the cooling process in the preparation of the materials.

4. A simple theoretical model has been developed to analyse the experimental data. It has been shown that higher heat expansion coefficients and lower heat conductivities correspond to lower densities and higher pore fractions for $V_g \gg V_p$. Lower densities not only produce higher residual stresses in quenching processes, but also, during annealing processes, provide larger releasing forces opposite to the residual stress produced by quenching.

5. Assuming that the magnetization process of the Ni–Cu–Zn ferrite is a rotation process, the stress was estimated by comparing the relative changes in the permeabilities of the unstressed and stressed samples. The stress obtained by the magnetic measurement agrees with the result of a mechanical test. The method used in our experiment provides a new non-destructive method of internal stress evaluation for ferroelectric and ferromagnetic ceramic materials.

6. Acknowledgements

This work was supported by the TDK Company, Japan. The authors would like to thank Mr S. Ito and Mr K. Kinoshita of TDK Ferrite Division and Mr S. Okamoto and Mr H. Moro of TDK Ferrite Research Center for their assistance in sample preparation and measurements. They also wish to thank A. Wang and S. C. Reising of the Department of Electrical Engineering of Washington University for their help and discussions.

References

1. G. MIAN and T. YAMAGUCHI, *J. Magn. Magn. Mater.* **68** (1987) 351.
2. J. SMITH, in "Magnetic Properties of Materials" (McGraw-Hill, New York, 1973) pp. 110–80.
3. S. CHIKAZUMI, in "Physics of Magnetism" (Robert E. Krieger Publishing, Malabar, FL, 1964) pp. 161–214.

Received 20 November 1989
and accepted 30 May 1990